INL/CON-10-19405
PREPRINT

ATR LEU Monolithic and Dispersed Fuel with ^{10}B Loading Minimization Design – Neutronics Performance Analysis

RERTR 2010

Gray S. Chang

October 2010

The INL is a
U.S. Department of Energy
National Laboratory
operated by
Battelle Energy Alliance

Attachment 3

RERTR 2010 — 32nd INTERNATIONAL MEETING ON REDUCED ENRICHMENT FOR RESEARCH AND TEST REACTORS

October 10-14, 2010
SANA Lisboa Hotel
Lisbon, Portugal

ATR LEU MONOLITHIC AND DISPERSED FUEL WITH ^{10}B LOADING MINIMIZATION DESIGN – NEUTRONICS PERFORMANCE ANALYSIS

Gray S. Chang
Idaho National Laboratory
2525 N. Fremont Ave.
Idaho Falls, ID 83415-3870
Email: gray.chang@inl.gov

ABSTRACT

The Advanced Test Reactor (ATR), currently operating in the United States, is used for material testing at very high neutron fluxes. Powered with highly enriched uranium (HEU), the ATR has a maximum thermal power rating of 250 MWth. Because of the large test volumes located in high flux areas, the ATR is an ideal candidate for assessing the feasibility of converting HEU driven reactor cores to low-enriched uranium (LEU) cores. The present work investigates the optimized LEU Monolithic and Dispersed fuel with ^{10}B loading minimization design and evaluates the subsequent neutronics operating effects of these optimized fuel designs.

The MCNP ATR 1/8th core model was used to optimize the ^{235}U and minimize the ^{10}B loading in the LEU core, such that the differences in K-eff and heat flux profiles between the HEU and LEU cores were minimized. The fuel depletion methodology MCWO was used to calculate K-eff versus effective full power days (EFPD) in this paper. The MCWO-calculated results for the optimized LEU Monolithic and Dispersed fuel cases demonstrated adequate excess reactivity such that the K-eff versus EFPD plot is similar to the ATR reference HEU case study.

Each HEU fuel element contains 19 fuel plates with a fuel meat thickness of 0.508 mm (20 mil). In this work, the proposed LEU Monolithic (U-10Mo) core conversion case with nominal fuel meat thickness of 0.330 mm (13 mil) and ^{235}U enrichment of 19.7 wt% is used to optimize the radial heat flux profile by varying the fuel meat thickness. The proposed LEU fuel meat varies from 0.203 mm (8.0 mil) to 0.254 mm (10.0 mil) at the inner four fuel plates (1-4) and outer four fuel plates (16-19). In addition, an optimized LEU dispersed (U7Mo) case with all the fuel meat thickness of 0.635 mm (25 mil) was also proposed. Then, for both Monolithic and dispersed cases, a burnable absorber – ^{10}B, was added in the inner and outer plates to reduce the initial excess reactivity, and the higher to average ratio of the inner/outer heat flux more effectively. The final minimized ^{10}B loading for LEU case studies will have 0.635 g in the LEU fuel meat at the inner 2 fuel plates (1-2) and outer 2 fuel plates (18-19), which can achieve peak to average ratios similar to those for the ATR reference HEU case study. The investigation of this paper shows the optimized LEU Monolithic (U-10Mo) and Dispersed (U7Mo) cases can all meet the LEU conversion objectives.

1. Introduction

The Advanced Test Reactor (ATR) at the Idaho National Laboratory (INL) is a high power density and high neutron flux research reactor operating in the United States. Powered with highly enriched uranium (HEU), the ATR has a maximum thermal power rating of 250 MW_{th} with a maximum unperturbed thermal neutron flux rating of 1.0×10^{15} n/cm^2–s. The conversion of nuclear test reactors currently fueled with HEU to operate with low-enriched uranium (LEU) is being addressed by the reduced enrichment for research and test reactors (RERTR) program. The ATR is a representative candidate for assessing the necessary modifications and evaluating the subsequent operating effects encountered when converting from HEU to LEU fuel.

The scope of this task is to assess the feasibility of converting the ATR HEU fuel to LEU fuel while retaining all key functional and safety characteristics of the reactor. Using the current HEU ^{235}U enrichment of 93.0 % as a baseline, this study will evaluate the LEU uranium density required in the fuel meat to yield an equivalent K-eff between the ATR HEU core and an LEU core after 125 effective full power days (EFPD) of operation with a total core power of 115 MW. A lobe power of 23 MW is assumed for each of the five lobes. Then, the LEU ^{235}U loading that yields an equivalent K-eff as the HEU ^{235}U loading will be used to predict radial, axial, and azimuthal power distributions. The heat rate distributions will also be evaluated for this core and used to predict the core performance as it relates to the current Upgraded Final Safety Analysis Report (UFSAR) and the associated Technical Safety Requirements (TSRs).

2. ATR MCNP Full Core Model Description

The ATR was originally commissioned in 1967 with the primary mission of materials and fuels testing for the United States Naval Reactors Program. The ATR is a high power density and high neutron flux research reactor with large test volumes in high flux regions. General characteristics for the ATR are listed in Table 1. Powered with HEU, the ATR has a maximum thermal power rating of 250 MW_{th} with a maximum unperturbed thermal neutron flux rating of 1.0×10^{15} n/cm^2–s.

The ATR was designed to provide large-volume, high-flux test locations. The unique serpentine fuel arrangement provides nine high-intensity neutron flux traps and 68 additional irradiation positions inside the reactor core reflector tank, each of which can contain multiple experiments.

The ATR has five lobes which are loosely coupled. These five lobes are identified as Northwest (NW), Northeast (NE), Center (C), Southwest (SW), and Southeast (SE). During full power operation, operators can maintain the desired lobe power by rotating the Outer Shim Control Cylinders (OSCC) and withdrawing/inserting the neck shim control rods. Each lobe within the ATR can be viewed as a quasi-independent reactor such that the ATR is virtually five smaller reactors. A Lobe-by-Lobe (LbyL) conversion strategy will be developed in order to minimize the impact to experiments within the other lobes.

Table 1. ATR general characteristics.

Reactor Parameter	Value
Thermal Power	250 MW_{th}[a]
Power Density	1.0 MW/L
Maximum Thermal Neutron Flux	1.0×10^{15} n/cm^2-s[b]
Maximum Fast Flux	5.0×10^{14} n/cm^2-s[b]
Number of Flux Traps	9
Number of Experiment Positions	68[c]
Core Parameter	**Value**
Number of Fuel Assemblies	40
Active Length of Assemblies	1.2 m (4 ft)
Number of Fuel Plates per Assembly	19
^{235}UContent of an Assembly	1,075 g
Total Core Fresh Fuel Load	43 kg
Coolant Parameter	**Value**
Design Pressure	0.7 MPa (390 psig)
Design Temperature	115°C (240°F)
Reactor Coolant	Light Water
Maximum Coolant Flow Rate	3.09 m^3/s (49,000 gpm)
Coolant Temperature, Inlet (Operating)	< 52°C (125°F) inlet
Coolant Temperature, Outlet (Operating)	71°C (160°F) outlet

a. Maximum design power of 250 MW. The ATR typically operates at a total core power of less than 115 MW.
b. These parameters are based on the full 250 MW power level and will be proportionally reduced for lower reactor power levels.
c. Only 66 of these positions are available for irradiation.

The detailed plate-by-plate MCNP ATR model was developed and generated as shown in Figure 1. The 40 fuel elements (FE) are explicitly modeled with 19 plates per FE. The ability to accurately predict K-eff and fission power distribution within the 19 fuel plates using the MCNP model is essential to the ATR LEU core conversion design. The detailed validation of the plate-by-plate MCNP ATR Full Core Model was presented in Ref. [1]. It was concluded that the ATR full core MCNP-calculated K-eff compared to the PDQ [2] model with respect to the Cycle 134A [3] ATR SUrveillance DAta System (ASUDAS) [4] data is in a very good agreement.

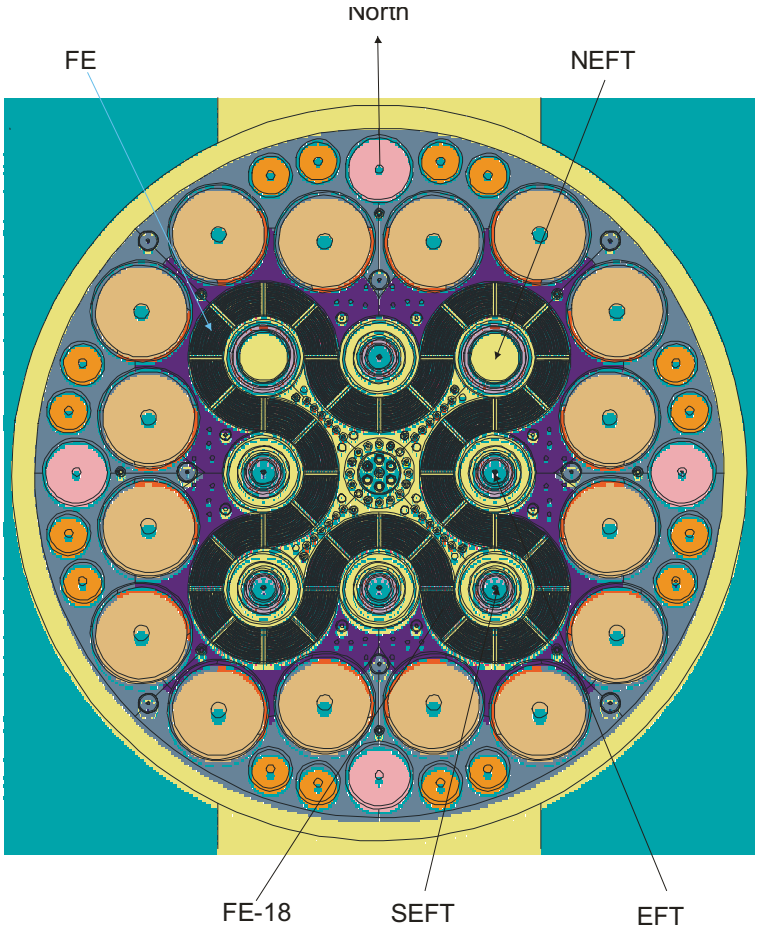

Figure 1. ATR MCNP full core model with 19 fuel plates per FE.

3. Plate-by-Plate ATR 1/8th Core Model for Fuel Burnup Analysis

A detailed plate-by-plate MCNP ATR 1/8th core model (Figure 2) was derived from the validated MCNP ATR full core model for the fuel cycle burnup analysis. The FE-18 details are shown in Figure 3. This model is used to optimize the ^{235}U and minimize ^{10}B loading in the LEU core by minimizing the K-eff differences with respect to the HEU core after 125 EFPD of operation with a total core power of 115 MW (23 MW per lobe).

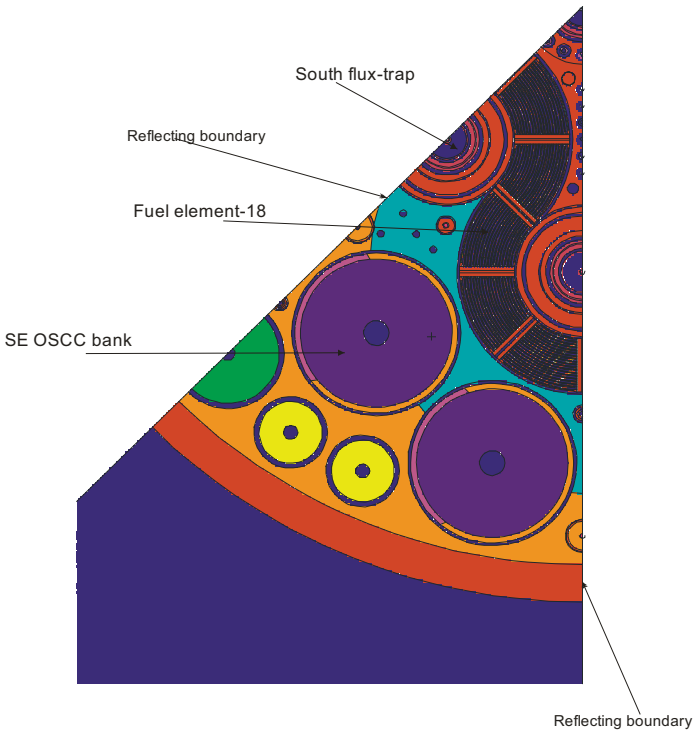

Figure 2. Detailed ATR SE-lobe 1/8th core MCNP model (FEs 16 – 20).

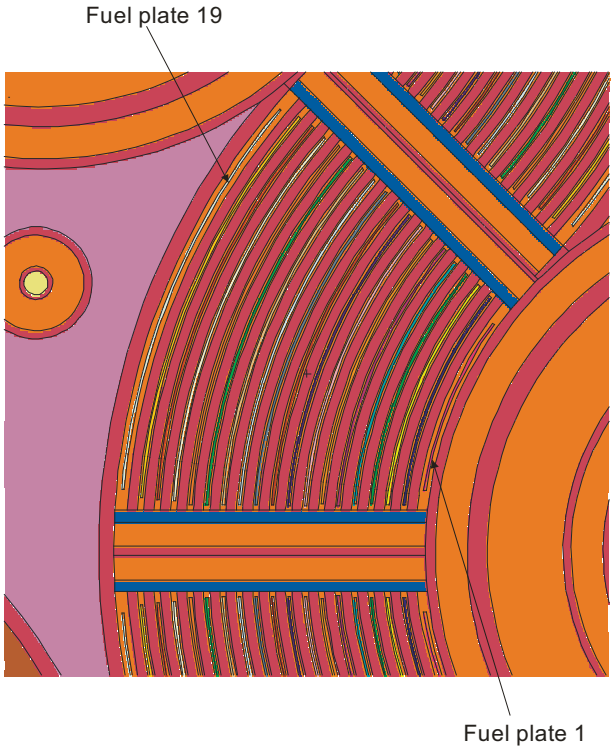

Figure 3. ATR MCNP model FE-18 detail.

4. MCWO – Fuel Burnup Analysis Tool

The fuel burnup analysis tool used in this study consists of a BASH (Bourne Again Shell) script file that links together the two FORTRAN data processing programs, m2o.f[5] and o2m.f. [5] This burnup methodology couples the Monte Carlo transport code MCNP [6,7] with the radioactive decay and burnup code ORIGEN2. [8] The methodology is known as Monte Carlo with ORIGEN2, or MCWO. [4,9]

The MCWO methodology produces criticality and burnup data based on various material feed/removal specifications, core power(s), and irradiation time intervals. MCWO processes user-specified input for geometry, initial material compositions, feed/removal specifications, and other problem-specific parameters.

The MCWO methodology uses MCNP-calculated one-group microscopic cross sections and fluxes as input to a series of ORIGEN2 burnup calculations. ORIGEN2 depletes/activates materials and generates isotopic compositions for subsequent MCNP calculations.

MCWO performs one MCNP and one or more ORIGEN2 calculations for each user-specified time step. Due to the highly time-dependent nature of the physics parameters and material compositions of the modeled reactor system, the MCWO-calculated results are typically more accurate if long irradiation cycles are broken up into smaller intervals. It should be noted that an increase in the number of ORIGEN2 calculation steps does not significantly impact the overall MCWO execution time because MCNP dominates the MCWO execution time.

For each MCNP calculation step, MCNP updates the fission power distribution and burnup-dependent cross sections for each fuel plate, then transfers the data to ORIGEN2 for cell-wise depletion calculations. The MCNP-generated reaction rates are integrated over the continuous-energy nuclear data and the space within the region.

5. Evaluation of ATR HEU Cases Fuel Neutronics Performances

ATR has four fuel element types, which are designated 7F, 7NB, 7NBH, and YA. [10] They are all versions of the zone loaded fuel element design and are identically constructed, varying only in the content of the fuel matrix. The 7F FE was chosen as the reference HEU Case-A in this study. Table 2 shows the nominal ^{235}U and ^{10}B loadings for each fuel plate of the 7F FE. In the 7F fuel element, all 19 fuel plates are loaded with 93% enriched uranium in an aluminum matrix to a total of 1075 g U-235. The eight outer plates (plate-1 to plate-4 and plate-16 to plate-19) contain boron as a burnable poison to a total of 0.66 g ^{10}B. To provide additional reactivity in certain locations, the 7NB fuel element, which is identical to the 7F fuel element, contains no burnable poison. For fuel cycle performance comparison, the 7NB fuel element was chosen as Case-A0 in this work.

Table 2. Specifications for a ATR reference HEU (^{235}U 93wt%) FE with B-10 in the 4 inner/outer fuel plates.

HEU Plate	Fuel Meat Thickness (mil)	Fuel Meat Volume (cc)	^{235}U Mass (g)	^{10}B Mass (g)	^{235}U Density (g/cc)
Plate-1	20	23.69	24.3	0.063	1.026
Plate-2	20	29.54	29.1	0.078	0.985
Plate-3	20	31.12	38.7	0.044	1.243
Plate-4	20	32.7	40.4	0.045	1.235
Plate-5	20	34.29	52.1	–	1.52
Plate-6	20	35.87	54.6	–	1.522
Plate-7	20	37.45	57	–	1.522
Plate-8	20	39.03	59.4	–	1.522
Plate-9	20	40.61	61.8	–	1.522
Plate-10	20	42.19	64.2	–	1.522
Plate-11	20	43.78	66.6	–	1.521
Plate-12	20	45.36	69	–	1.521
Plate-13	20	46.94	71.4	–	1.521
Plate-14	20	48.52	73.8	–	1.521
Plate-15	20	50.1	76.3	–	1.523
Plate-16	20	51.69	64	0.071	1.238
Plate-17	20	53.27	65.9	0.073	1.237
Plate-18	20	54.22	53.8	0.143	0.992
Plate-19	20	52.64	52.6	0.143	0.999
Total		792.99	1075	0.66	–

ATR MCNP detailed 1/8th core model was used to perform the evaluation of the ATR reference HEU cases with and without burnable absorber ^{10}B at the beginning of cycle (BOC) condition. Then, MCWO was used to evaluate the fuel cycle performance versus the EFPD for the following cases: The fuel burnup analysis assumed that each nominal operating cycle was 50 EFPD followed immediately by a seven day outage. Each 50 EFPD cycle was subdivided into 5 EFPD time step intervals. The OSCC positions were set to 105°. The resultant MCNP-calculated tallies were normalized to a south lobe source power of 23 MW.

5.1 Comparison of K-eff versus EFPD for ATR Reference 7F Fuel (Case-A) and 7NB Fuel (Case-A0)

The MCWO-calculated K-eff for HEU Case-A and Case-A0 are plotted in Figure 4. Note that at the beginning of cycle (BOC) for each of the three nominal operating cycles modeled, the initial Xe poison was set to zero or decayed to a very small value during the 7 day shutdown time, thus causing a jump increase in K-eff. The MCWO-calculated results of the K-eff versus EFPD for Case-A and Case-A0 demonstrates that the ATR HEU fuel provides the same adequate excess

reactivity (for K-eff larger than one) for about 150 EFPD of reactor power operation. The K-eff of Case-A and Case-A0 at BOC are 1.1131 and 1.2069, respectively, which represents a hold-down reactivity of $10.16 for the delayed neutron fraction (β) of 0.0069.

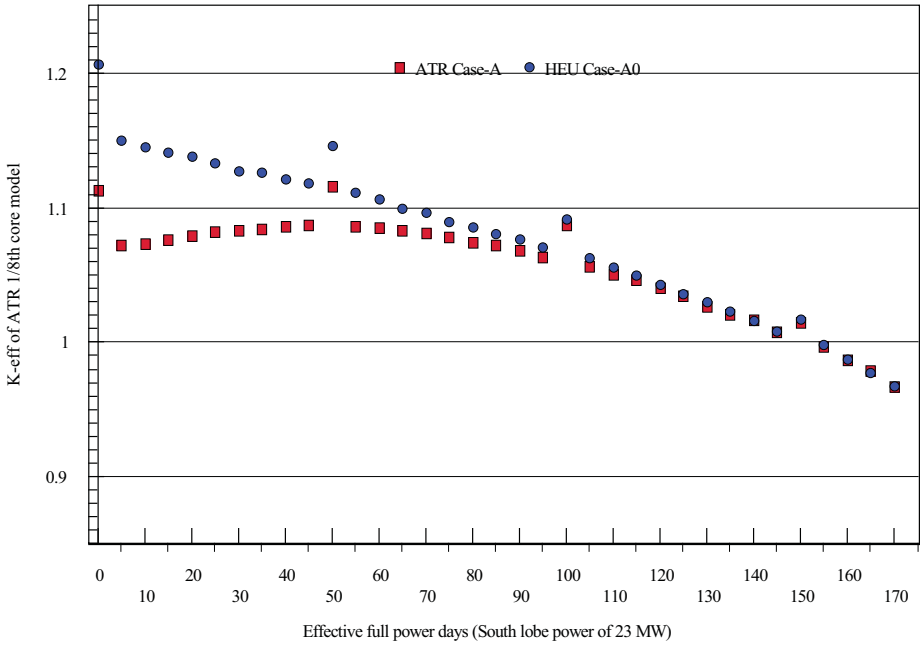

Figure 4. K-eff vs. EFPD for ATR reference HEU Case-A and Case-A0.

5.2 Comparison of Radial Fission Power Profiles at BOC for ATR HUE Case-A1 and Case-A0

For the beginning of the first irradiation cycle, the relative radial fuel plate fission power heat fluxes were calculated for Case-A1 and Case-A0 and the results for FE-18 are plotted in Figure 5. For the ATR reference HEU Case-A, the 4 inner/outer plates (plate-1 to plate-4and plate-16 to plate-19) are loaded with 0.66 g of ^{10}B, a burnable absorber, which flattens the relative heat flux local-to-average-ratio (L2RA) in the inner/outer plates to a peak value of about 1.25. Case-A0 does not have any burnable absorber in the 4 inner/outer fuel plates, therefore the peak relative heat flux L2RA is approximately 1.31. From the above discussions, we conclude that the burnable absorber ^{10}B not only can effectively hold-down the initial excess reactivity, but also can reduce the peak relative heat flux L2RA from 1.31 to 1.25.

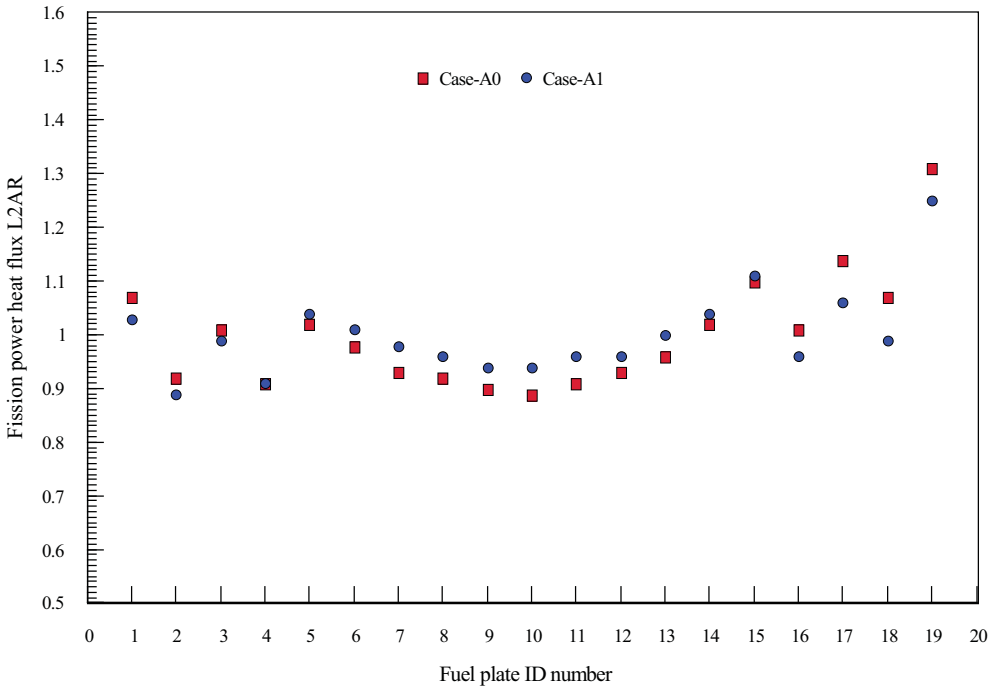

Figure 5. Radial fission power heat flux L2AR for ATR reference HEU Case-A, and Case-A0.

6. LEU Monolithic and Dispersed Fuel Specification and ^{10}B Loading Minimization Neutronics Performance Evaluation

An optimized LEU monolithic fuel design with varied fuel meat thickness in the four inner plates (plate-1 to plate-4) and four outer plates (plate-16 to plate-19) was recommended in Ref. [1]. However, those optimized LEU fuel designs did not include the ^{10}B loading minimization. Because the ^{10}B (n,α) reaction will produce Helium-4 (He-4), which can degrade the LEU foil fuel (U10Mo) type fuel performance, an alternative burnable absorber loading option is proposed in this study. Since the LEU dispersed fuel (U7Mo) type has a much better tolerance with respect to ^{10}B during fuel burnup, its design and neutronics performance evaluation was also included in this work.

The optimization was based upon a comparison of the MCWO-calculated K-eff versus EFPD and the radial power L2AR profile for various LEU fuel and ^{10}B loading schemes. In order to reduce the ^{10}B depletion impact on the fuel plate performance, ^{10}B was modeled in the two inner plates (plate-1 and plate-2) and two outer plates (plate-18 and plate-19). The LEU fuel (^{235}U enrichment 19.7wt%) loading schemes included varying parameters such as fuel meat thickness within the monolithic U10-Mo LEU fuel type as Case-B. For Case-C, the LEU dispersed (U7Mo) fuel type, the ^{235}U loading in the inner and outer four plates was varied. Based upon the comparison between Case-A , Case-B, and Case-C relative heat flux L2AR profiles, the ^{235}U contents and fuel meat thickness of the inner/outer plates were evaluated and optimized in order to reduce the difference of K-eff profiles versus EFPD and LEU fuel peak heat flux L2AR. The LEU fuel loading was optimized such that the L2AR at the four inner/outer plates closely matches the ATR reference HEU Case-A. The optimization was achieved by reducing the fuel

meat thickness as well as loading the two inner/outer plates with 0.63 g of ^{10}B, LEU Case-B and Case-C. The optimized LEU fuel plate specifications for Case-B and Case-C are given in Table 3 and Table 4, respectively. Table 3 shows that the nominal fuel meat thickness is 0.0330 cm (13 mil). The varied four inner plates (plate-1 to plate-4) fuel meat thicknesses are 0.0203 cm (8 mil), 0.0203 cm (8 mil), 0.0354 cm (10 mil), and 0.0305 cm (12 mil), respectively. While the varied 4 outer plates (plate-16 to plate-19) fuel meat thicknesses are 0.0305 cm (12 mil), 0.0354 cm (10 mil), 0.0203 cm (8 mil), and 0.0203 cm (8 mil), respectively. For the dispersed fuel type, Table 4 shows that all fuel meat thicknesses are 0.0635 cm (25 mil). The nominal ^{235}U loading density for fuel plates is 1.48 g/cc. The varied ^{235}U loading density for the inner plates-1 to -3 are 1.08, 1.18, and 1.38 g/cc, respectively. And, the varied ^{235}U loading density for the inner plates-17 to -19 are 1.28, 1.18, and 0.99 g/cc, respectively.

Table 3. Optimized LEU Case B (U10Mo) monolithic fuel specification.

LEU Plate	Fuel Meat Thickness (mil)	Fuel meat Vol. (cc)	U-235 Mass (g)	Boron_10 Mass (g)	U-235 Density (g/cc)
Plate-1	8	9.47	28.57	0.058	3.02
Plate-2	8	11.82	35.68	0.149	3.02
Plate-3	10	15.51	46.81	0	3.02
Plate-4	12	16.29	49.16	0	3.02
Plate-5	13	22.18	66.94	0	3.02
Plate-6	13	23.66	71.4	0	3.02
Plate-7	13	24.71	74.57	0	3.02
Plate-8	13	25.75	77.7	0	3.02
Plate-9	13	26.8	80.87	0	3.02
Plate-10	13	27.82	83.97	0	3.02
Plate-11	13	28.89	87.19	0	3.02
Plate-12	13	29.92	90.31	0	3.02
Plate-13	13	30.97	93.47	0	3.02
Plate-14	13	32.01	96.6	0	3.02
Plate-15	13	33.07	99.79	0	3.02
Plate-16	12	25.74	77.69	0	3.02
Plate-17	10	26.53	80.07	0	3.02
Plate-18	8	21.7	65.49	0.111	3.02
Plate-19	8	21.49	64.85	0.317	3.02
Total		454.33	1371.13	0.636	

Table 4. Optimized LEU Case-C (U7Mo) dispersed fuel specification. (All fuel meat thicknesses are 25 mil.)

LEU Plate ID	Fuel Meat Total U g/cc	Fuel meat Vol. (cc)	U-235 Mass (g)	Boron_10 Mass (g)	U-235 Density (g/cc)
Plate-1	5.5	29.49	31.96	0.058	1.08
Plate-2	6	36.84	43.54	0.149	1.18
Plate-3	7	38.80	53.51	0	1.38
Plate-4	7.5	40.77	60.24	0	1.48
Plate-5	7.5	42.73	63.13	0	1.48
Plate-6	7.5	45.57	67.32	0	1.48
Plate-7	7.5	47.59	70.31	0	1.48
Plate-8	7.5	49.58	73.25	0	1.48
Plate-9	7.5	51.60	76.24	0	1.48
Plate-10	7.5	53.59	79.18	0	1.48
Plate-11	7.5	55.63	82.19	0	1.48
Plate-12	7.5	57.62	85.13	0	1.48
Plate-13	7.5	59.63	88.11	0	1.48
Plate-14	7.5	61.63	91.06	0	1.48
Plate-15	7.5	63.66	94.05	0	1.48
Plate-16	7.5	64.40	95.15	0	1.48
Plate-17	6.5	66.38	84.99	0	1.28
Plate-18	6	67.57	79.87	0.111	1.18
Plate-19	5	66.94	65.94	0.317	0.99
Total		1000.01	1385.18	0.636	

6.1 Optimized LEU Radial Fission Power Profile at BOC

The above Table 3 and Table 4 summarize the fuel and ^{10}B minimization loading parameter variations that resulted in the flattest radial fission heat profile while still maintaining sufficient reactivity within the LEU core. Not surprisingly, the optimal LEU fuel loading is similar to the HEU reference case. The optimal LEU fuel loading has thinner plates at the inner/outer plate positions. For the purposes of determining the feasibility of HEU to LEU conversion, however, the present study demonstrates a satisfactory loading scheme to achieve acceptable reactivity for three nominal 50 EFPD fuel cycles as well as maintain the radial heat flux L2AR profile.

The MCWO fuel burnup analysis code was used to calculate the relative radial plate fission power heat flux for the optimized LEU cases for the beginning of the first cycle (Case-A1, Case-B1, and Case-C1). In FE-18, the respective peak heat fluxes L2AR for Case-A1, Casae-B1, and Case-C1 were determined to be 1.25, 1.21, and 1.20, respectively. Results for Case-A1, Case-B1, and Case-C1 are plotted in Figure 6. This plot demonstrates that Case-B and Case-C yield very similar radial L2AR profiles as compared to Case-A.

These studies indicate that the LEU radial L2AR profiles can achieve flattened profiles bounded by HEU reference Case-A by varying fuel meat thickness of the inner/outer 4 plates. Although,

the fission power density (W/cm^3) L2AR profiles for the LEU cases with varied fuel meat thickness produced larger peaks within the inner/outer plates. This power density peaking will not result in a large, undesirable heat flux profile.

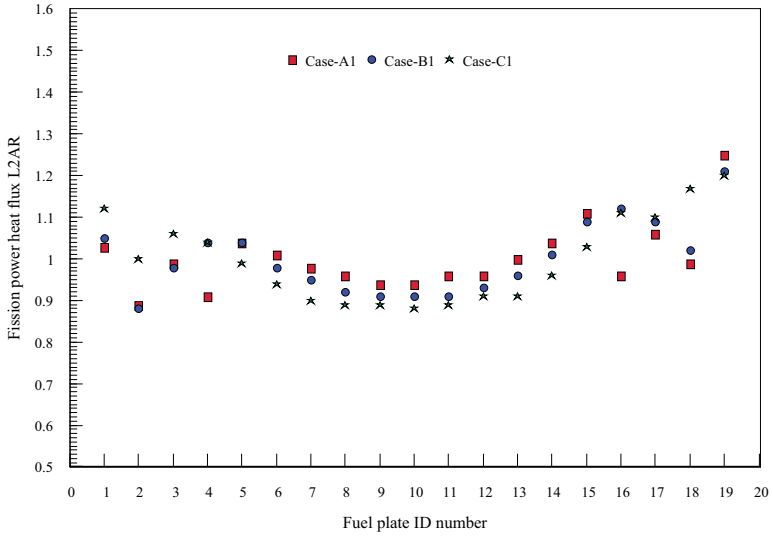

Figure 6. Fission power heat flux L2AR radial profiles for HEU Case-A and optimized LEU Case-B and Case-C.

6.2 Optimized LEU Cases K-eff versus EFPD

Using the optimized LEU fuel loading, the MCWO-calculated K-eff for LEU Case-A and Case-B as a function of EFPD as compared to the ATR reference HEU Case-A is shown in Figure 7. Note that the LEU fuels contain 80.3 wt% U-238, which can be transmuted to Pu-239. Although the LEU cases have a lower K-eff at the BOC when compared with HEU Case-A, the LEU cases sustain operation for the same EFPD as HEU Case-A (150 EFPD). The K-eff of Case-B and Case-B without ^{10}B at BOC are 1.0767 and 1.1461, respectively, which represents a hold-down reactivity of \$8.15. For the dispersed fuel type, the K-eff of Case-C and Case-C without ^{10}B at BOC are 1.0725 and 1.1513, respectively, which represents a hold-down reactivity of \$9.25.

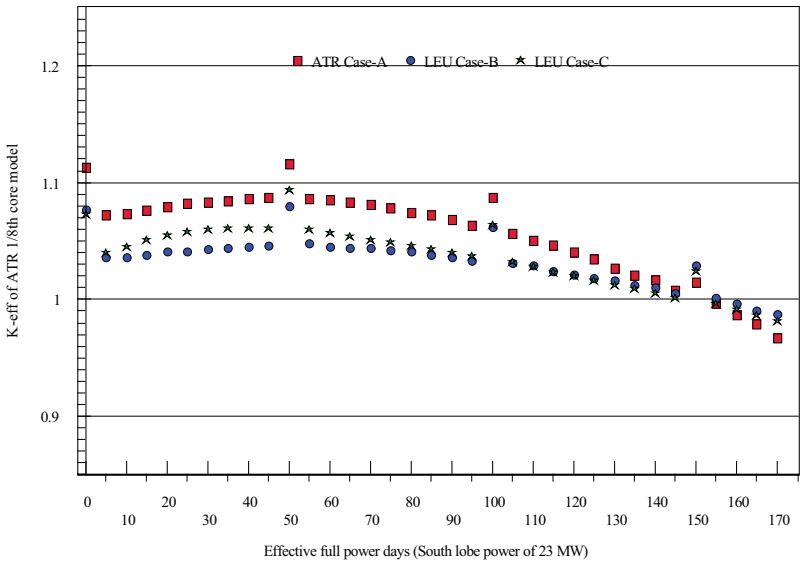

Figure 7. MCWO-calculated K-3ff versus EFPD for ATR reference HEU Case-A and optimized LEU Case-B and Case-C.

7. Conclusion and Recommendations

The detailed plate-by-plate MCNP ATR 1/8th core model used in this study handles complex spectral transitions at the boundaries between the plates in a straight forward manner. The MCWO-calculated K-eff versus EFPD results indicate that both LEU Case-B and Case-C provide excess reactivity versus burnup while providing fission heat profiles similar to the ATR reference HEU Case-A. The LEU core conversion designer will be able to optimize the ^{235}U fuel loading so that the K-eff and relative radial fission heat flux profile are similar to Case-A. To achieve the flattened heat flux profile, the LEU monolithic core designer can fix the ^{235}U enrichment of 19.7wt% and vary the thickness of the four inner/outer plates, as well as adjust the amount of burnable absorber in the two inner/outer plates. The LEU dispersed core designer can also fix the ^{235}U enrichment of 19.7wt% and vary the ^{235}U loading of the four inner/outer plates, as well as adjust the amount of burnable absorber in the two inner/outer plates. The investigation of this paper shows the optimized LEU Monolithic (U-10Mo) and Dispersed (U7Mo) cases can all meet the LEU conversion objectives. As a result, it has been concluded that LEU core conversion for the ATR is feasible.

The LEU core designer can use the detailed plate-by-plate MCNP ATR 1/8th core model to optimize the ^{235}U loading by either minimizing K-eff differences with respect to the HEU core during the 150 EFPD of operation at a total core power of 115 MW (23 MW per lobe), or by reducing the higher L2AR of heat flux at the inner/outer plates. However, to demonstrate that the LEU core fuel cycle performance can meet the UFSAR safety requirement, a further study will be necessary in order to investigate the detailed radial, axial, and azimuthal heat flux profile variations versus EFPD.

To demonstrate that the LEU core fuel cycle performance can meet the Updated Final Safety Analysis Report (UFSAR) safety requirements, additional studies will be necessary to evaluate and compare safety parameters such as void reactivity and Doppler coefficients, control components worth (outer shim control cylinders, safety rods and regulating rod), and shutdown margins between the HEU and LEU cores.

8. References

[1] G. S. Chang, M. A. Lillo, R. G. Ambrosek (retired), 'Neutronics and Thermal Hydraulics Study for Using a Low-Enriched Uranium Core in the Advanced Test Reactor 2008 Final Report,' INL/EXT-08-13980, June 2008.

[2] Roth, P. A., 2004a, letter to J. D. Abrashoff, PAR-17-04, revision 1, "Startup Outer Shim Prediction for ATR Cycle 134A-1, Revision 1," December 20, 2004.

[3] ASUDAS report from DAC Hourly Control History for Cycle 134A-1/A-2 End of Cycle; provided by email from D. V. Thomas to M. A. Lillo, July 11, 2005.

[4] Cook W. C., Smith A. C., "ATR CSAP Package on the Workstation Version 1," PG-T-96-002, May, 1996.

[5] G. S. Chang, "MCWO - LINKING MCNP AND ORIGEN2 FOR FUEL BURNUP ANALYSIS," Proceedings of 'The Monte Carlo Method: Versatility Unbounded In A Dynamic Computing World,' Chattanooga, Tennessee, April 17–21, 2005, on CD-ROM, American Nuclear Society, LaGrange Park, IL (2005).

[6] Tim Goorley, Jeff Bull, Forrest Brown, et. al., "Release of MCNP5_RSICC_1.30," MCNP Monte Carlo Team X-5, LA-UR-04-4519, Los Alamos National Laboratory, November 2004.

[7] X-5 Monte Carlo Team, "MCNP—A General Monte Carlo N-Particle Transport Code, Version 5," Volume I (LA-UR-03-1987) and Volume II (LA-CP-0245), Los Alamos National Laboratory April 24, 2003 (Revised 6/30/2004).

[8] G. Croff, "ORIGEN2: A Versatile Computer Code for Calculating the Nuclide Compositions and Characteristics of Nuclear Materials, Nuclear Technology," Vol. 62, pp. 335-352, 1983.

[9] G. S. Chang and J. M. Ryskamp, "Depletion Analysis of Mixed Oxide Fuel Pins in Light Water Reactors and the Advanced Test Reactor," Nucl. Technol., Vol. 129, No. 3, p. 326-337 (2000).

[10] Safety Analysis Report, "Safety Analysis Report for the Advanced Test Reactor," Idaho National Laboratory, SAR-153, Nov. 2003.